

# Study of the $Y(4260)$ resonance in $e^+e^-$ collisions with initial state radiation at Belle

K. Abe,<sup>9</sup> K. Abe,<sup>49</sup> I. Adachi,<sup>9</sup> H. Aihara,<sup>51</sup> D. Anipko,<sup>1</sup> K. Aoki,<sup>25</sup> T. Arakawa,<sup>32</sup>  
 K. Arinstein,<sup>1</sup> Y. Asano,<sup>56</sup> T. Aso,<sup>55</sup> V. Aulchenko,<sup>1</sup> T. Aushev,<sup>21</sup> T. Aziz,<sup>47</sup> S. Bahinipati,<sup>4</sup>  
 A. M. Bakich,<sup>46</sup> V. Balagura,<sup>15</sup> Y. Ban,<sup>37</sup> S. Banerjee,<sup>47</sup> E. Barberio,<sup>24</sup> M. Barbero,<sup>8</sup>  
 A. Bay,<sup>21</sup> I. Bedny,<sup>1</sup> K. Belous,<sup>14</sup> U. Bitenc,<sup>16</sup> I. Bizjak,<sup>16</sup> S. Blyth,<sup>27</sup> A. Bondar,<sup>1</sup>  
 A. Bozek,<sup>30</sup> M. Bračko,<sup>23,16</sup> J. Brodzicka,<sup>9,30</sup> T. E. Browder,<sup>8</sup> M.-C. Chang,<sup>50</sup> P. Chang,<sup>29</sup>  
 Y. Chao,<sup>29</sup> A. Chen,<sup>27</sup> K.-F. Chen,<sup>29</sup> W. T. Chen,<sup>27</sup> B. G. Cheon,<sup>3</sup> R. Chistov,<sup>15</sup>  
 J. H. Choi,<sup>18</sup> S.-K. Choi,<sup>7</sup> Y. Choi,<sup>45</sup> Y. K. Choi,<sup>45</sup> A. Chuvikov,<sup>39</sup> S. Cole,<sup>46</sup> J. Dalseno,<sup>24</sup>  
 M. Danilov,<sup>15</sup> M. Dash,<sup>57</sup> R. Dowd,<sup>24</sup> J. Dragic,<sup>9</sup> A. Drutskoy,<sup>4</sup> S. Eidelman,<sup>1</sup> Y. Enari,<sup>25</sup>  
 D. Epifanov,<sup>1</sup> S. Fratina,<sup>16</sup> H. Fujii,<sup>9</sup> M. Fujikawa,<sup>26</sup> N. Gabyshev,<sup>1</sup> A. Garmash,<sup>39</sup>  
 T. Gershon,<sup>9</sup> A. Go,<sup>27</sup> G. Gokhroo,<sup>47</sup> P. Goldenzweig,<sup>4</sup> B. Golob,<sup>22,16</sup> A. Gorišek,<sup>16</sup>  
 M. Grosse Perdekamp,<sup>11,40</sup> H. Guler,<sup>8</sup> H. Ha,<sup>18</sup> J. Haba,<sup>9</sup> K. Hara,<sup>25</sup> T. Hara,<sup>35</sup>  
 Y. Hasegawa,<sup>44</sup> N. C. Hastings,<sup>51</sup> K. Hayasaka,<sup>25</sup> H. Hayashii,<sup>26</sup> M. Hazumi,<sup>9</sup>  
 D. Heffernan,<sup>35</sup> T. Higuchi,<sup>9</sup> L. Hinz,<sup>21</sup> T. Hokuue,<sup>25</sup> Y. Hoshi,<sup>49</sup> K. Hoshina,<sup>54</sup> S. Hou,<sup>27</sup>  
 W.-S. Hou,<sup>29</sup> Y. B. Hsiung,<sup>29</sup> Y. Igarashi,<sup>9</sup> T. Iijima,<sup>25</sup> K. Ikado,<sup>25</sup> A. Imoto,<sup>26</sup> K. Inami,<sup>25</sup>  
 A. Ishikawa,<sup>51</sup> H. Ishino,<sup>52</sup> K. Itoh,<sup>51</sup> R. Itoh,<sup>9</sup> M. Iwabuchi,<sup>6</sup> M. Iwasaki,<sup>51</sup> Y. Iwasaki,<sup>9</sup>  
 C. Jacoby,<sup>21</sup> M. Jones,<sup>8</sup> H. Kakuno,<sup>51</sup> J. H. Kang,<sup>58</sup> J. S. Kang,<sup>18</sup> P. Kapusta,<sup>30</sup>  
 S. U. Kataoka,<sup>26</sup> N. Katayama,<sup>9</sup> H. Kawai,<sup>2</sup> T. Kawasaki,<sup>32</sup> H. R. Khan,<sup>52</sup> A. Kibayashi,<sup>52</sup>  
 H. Kichimi,<sup>9</sup> N. Kikuchi,<sup>50</sup> H. J. Kim,<sup>20</sup> H. O. Kim,<sup>45</sup> J. H. Kim,<sup>45</sup> S. K. Kim,<sup>43</sup>  
 T. H. Kim,<sup>58</sup> Y. J. Kim,<sup>6</sup> K. Kinoshita,<sup>4</sup> N. Kishimoto,<sup>25</sup> S. Korpar,<sup>23,16</sup> Y. Kozakai,<sup>25</sup>  
 P. Križan,<sup>22,16</sup> P. Krokovny,<sup>9</sup> T. Kubota,<sup>25</sup> R. Kulasiri,<sup>4</sup> R. Kumar,<sup>36</sup> C. C. Kuo,<sup>27</sup>  
 E. Kurihara,<sup>2</sup> A. Kusaka,<sup>51</sup> A. Kuzmin,<sup>1</sup> Y.-J. Kwon,<sup>58</sup> J. S. Lange,<sup>5</sup> G. Leder,<sup>13</sup> J. Lee,<sup>43</sup>  
 S. E. Lee,<sup>43</sup> Y.-J. Lee,<sup>29</sup> T. Lesiak,<sup>30</sup> J. Li,<sup>8</sup> A. Limosani,<sup>9</sup> C. Y. Lin,<sup>29</sup> S.-W. Lin,<sup>29</sup>  
 Y. Liu,<sup>6</sup> D. Liventsev,<sup>15</sup> J. MacNaughton,<sup>13</sup> G. Majumder,<sup>47</sup> F. Mandl,<sup>13</sup> D. Marlow,<sup>39</sup>  
 T. Matsumoto,<sup>53</sup> A. Matyja,<sup>30</sup> S. McOnie,<sup>46</sup> T. Medvedeva,<sup>15</sup> Y. Mikami,<sup>50</sup> W. Mitaroff,<sup>13</sup>  
 K. Miyabayashi,<sup>26</sup> H. Miyake,<sup>35</sup> H. Miyata,<sup>32</sup> Y. Miyazaki,<sup>25</sup> R. Mizuk,<sup>15</sup> D. Mohapatra,<sup>57</sup>  
 G. R. Moloney,<sup>24</sup> T. Mori,<sup>52</sup> J. Mueller,<sup>38</sup> A. Murakami,<sup>41</sup> T. Nagamine,<sup>50</sup> Y. Nagasaka,<sup>10</sup>  
 T. Nakagawa,<sup>53</sup> Y. Nakahama,<sup>51</sup> I. Nakamura,<sup>9</sup> E. Nakano,<sup>34</sup> M. Nakao,<sup>9</sup> H. Nakazawa,<sup>9</sup>  
 Z. Natkaniec,<sup>30</sup> K. Neichi,<sup>49</sup> S. Nishida,<sup>9</sup> K. Nishimura,<sup>8</sup> O. Nitoh,<sup>54</sup> S. Noguchi,<sup>26</sup>  
 T. Nozaki,<sup>9</sup> A. Ogawa,<sup>40</sup> S. Ogawa,<sup>48</sup> T. Ohshima,<sup>25</sup> T. Okabe,<sup>25</sup> S. Okuno,<sup>17</sup> S. L. Olsen,<sup>8</sup>  
 S. Ono,<sup>52</sup> W. Ostrowicz,<sup>30</sup> H. Ozaki,<sup>9</sup> P. Pakhlov,<sup>15</sup> G. Pakhlova,<sup>15</sup> H. Palka,<sup>30</sup>  
 C. W. Park,<sup>45</sup> H. Park,<sup>20</sup> K. S. Park,<sup>45</sup> N. Parslow,<sup>46</sup> L. S. Peak,<sup>46</sup> M. Pernicka,<sup>13</sup>  
 R. Pestotnik,<sup>16</sup> M. Peters,<sup>8</sup> L. E. Piilonen,<sup>57</sup> A. Poluektov,<sup>1</sup> F. J. Ronga,<sup>9</sup> N. Root,<sup>1</sup>  
 J. Rorie,<sup>8</sup> M. Rozanska,<sup>30</sup> H. Sahoo,<sup>8</sup> S. Saitoh,<sup>9</sup> Y. Sakai,<sup>9</sup> H. Sakamoto,<sup>19</sup> H. Sakaue,<sup>34</sup>  
 T. R. Sarangi,<sup>6</sup> N. Sato,<sup>25</sup> N. Satoyama,<sup>44</sup> K. Sayeed,<sup>4</sup> T. Schietinger,<sup>21</sup> O. Schneider,<sup>21</sup>  
 P. Schönmeier,<sup>50</sup> J. Schümann,<sup>28</sup> C. Schwanda,<sup>13</sup> A. J. Schwartz,<sup>4</sup> R. Seidl,<sup>11,40</sup> T. Seki,<sup>53</sup>  
 K. Senyo,<sup>25</sup> M. E. Sevier,<sup>24</sup> M. Shapkin,<sup>14</sup> Y.-T. Shen,<sup>29</sup> H. Shibuya,<sup>48</sup> B. Shwartz,<sup>1</sup>  
 V. Sidorov,<sup>1</sup> J. B. Singh,<sup>36</sup> A. Sokolov,<sup>14</sup> A. Somov,<sup>4</sup> N. Soni,<sup>36</sup> R. Stamen,<sup>9</sup> S. Stanić,<sup>33</sup>  
 M. Starić,<sup>16</sup> H. Stoeck,<sup>46</sup> A. Sugiyama,<sup>41</sup> K. Sumisawa,<sup>9</sup> T. Sumiyoshi,<sup>53</sup> S. Suzuki,<sup>41</sup>  
 S. Y. Suzuki,<sup>9</sup> O. Tajima,<sup>9</sup> N. Takada,<sup>44</sup> F. Takasaki,<sup>9</sup> K. Tamai,<sup>9</sup> N. Tamura,<sup>32</sup>

K. Tanabe,<sup>51</sup> M. Tanaka,<sup>9</sup> G. N. Taylor,<sup>24</sup> Y. Teramoto,<sup>34</sup> X. C. Tian,<sup>37</sup> I. Tikhomirov,<sup>15</sup>  
 K. Trabelsi,<sup>9</sup> Y. T. Tsai,<sup>29</sup> Y. F. Tse,<sup>24</sup> T. Tsuboyama,<sup>9</sup> T. Tsukamoto,<sup>9</sup> K. Uchida,<sup>8</sup>  
 Y. Uchida,<sup>6</sup> S. Uehara,<sup>9</sup> T. Uglov,<sup>15</sup> K. Ueno,<sup>29</sup> Y. Unno,<sup>9</sup> S. Uno,<sup>9</sup> P. Urquijo,<sup>24</sup>  
 Y. Ushiroda,<sup>9</sup> Y. Usov,<sup>1</sup> G. Varner,<sup>8</sup> K. E. Varvell,<sup>46</sup> S. Villa,<sup>21</sup> C. C. Wang,<sup>29</sup>  
 C. H. Wang,<sup>28</sup> M.-Z. Wang,<sup>29</sup> M. Watanabe,<sup>32</sup> Y. Watanabe,<sup>52</sup> J. Wicht,<sup>21</sup> L. Widhalm,<sup>13</sup>  
 J. Wiechczynski,<sup>30</sup> E. Won,<sup>18</sup> C.-H. Wu,<sup>29</sup> Q. L. Xie,<sup>12</sup> B. D. Yabsley,<sup>46</sup> A. Yamaguchi,<sup>50</sup>  
 H. Yamamoto,<sup>50</sup> S. Yamamoto,<sup>53</sup> Y. Yamashita,<sup>31</sup> M. Yamauchi,<sup>9</sup> Heyoung Yang,<sup>43</sup>  
 S. Yoshino,<sup>25</sup> Y. Yuan,<sup>12</sup> Y. Yusa,<sup>57</sup> S. L. Zang,<sup>12</sup> C. C. Zhang,<sup>12</sup> J. Zhang,<sup>9</sup>  
 L. M. Zhang,<sup>42</sup> Z. P. Zhang,<sup>42</sup> V. Zhilich,<sup>1</sup> T. Ziegler,<sup>39</sup> A. Zupanc,<sup>16</sup> and D. Zürcher<sup>21</sup>

(The Belle Collaboration)

<sup>1</sup>*Budker Institute of Nuclear Physics, Novosibirsk*

<sup>2</sup>*Chiba University, Chiba*

<sup>3</sup>*Chonnam National University, Kwangju*

<sup>4</sup>*University of Cincinnati, Cincinnati, Ohio 45221*

<sup>5</sup>*University of Frankfurt, Frankfurt*

<sup>6</sup>*The Graduate University for Advanced Studies, Hayama*

<sup>7</sup>*Gyeongsang National University, Chinju*

<sup>8</sup>*University of Hawaii, Honolulu, Hawaii 96822*

<sup>9</sup>*High Energy Accelerator Research Organization (KEK), Tsukuba*

<sup>10</sup>*Hiroshima Institute of Technology, Hiroshima*

<sup>11</sup>*University of Illinois at Urbana-Champaign, Urbana, Illinois 61801*

<sup>12</sup>*Institute of High Energy Physics,*

*Chinese Academy of Sciences, Beijing*

<sup>13</sup>*Institute of High Energy Physics, Vienna*

<sup>14</sup>*Institute of High Energy Physics, Protvino*

<sup>15</sup>*Institute for Theoretical and Experimental Physics, Moscow*

<sup>16</sup>*J. Stefan Institute, Ljubljana*

<sup>17</sup>*Kanagawa University, Yokohama*

<sup>18</sup>*Korea University, Seoul*

<sup>19</sup>*Kyoto University, Kyoto*

<sup>20</sup>*Kyungpook National University, Taegu*

<sup>21</sup>*Swiss Federal Institute of Technology of Lausanne, EPFL, Lausanne*

<sup>22</sup>*University of Ljubljana, Ljubljana*

<sup>23</sup>*University of Maribor, Maribor*

<sup>24</sup>*University of Melbourne, Victoria*

<sup>25</sup>*Nagoya University, Nagoya*

<sup>26</sup>*Nara Women's University, Nara*

<sup>27</sup>*National Central University, Chung-li*

<sup>28</sup>*National United University, Miao Li*

<sup>29</sup>*Department of Physics, National Taiwan University, Taipei*

<sup>30</sup>*H. Niewodniczanski Institute of Nuclear Physics, Krakow*

<sup>31</sup>*Nippon Dental University, Niigata*

<sup>32</sup>*Niigata University, Niigata*

<sup>33</sup>*University of Nova Gorica, Nova Gorica*

<sup>34</sup>*Osaka City University, Osaka*

<sup>35</sup>*Osaka University, Osaka*

- <sup>36</sup>*Panjab University, Chandigarh*  
<sup>37</sup>*Peking University, Beijing*  
<sup>38</sup>*University of Pittsburgh, Pittsburgh, Pennsylvania 15260*  
<sup>39</sup>*Princeton University, Princeton, New Jersey 08544*  
<sup>40</sup>*RIKEN BNL Research Center, Upton, New York 11973*  
<sup>41</sup>*Saga University, Saga*  
<sup>42</sup>*University of Science and Technology of China, Hefei*  
<sup>43</sup>*Seoul National University, Seoul*  
<sup>44</sup>*Shinshu University, Nagano*  
<sup>45</sup>*Sungkyunkwan University, Suwon*  
<sup>46</sup>*University of Sydney, Sydney NSW*  
<sup>47</sup>*Tata Institute of Fundamental Research, Bombay*  
<sup>48</sup>*Toho University, Funabashi*  
<sup>49</sup>*Tohoku Gakuin University, Tagajo*  
<sup>50</sup>*Tohoku University, Sendai*  
<sup>51</sup>*Department of Physics, University of Tokyo, Tokyo*  
<sup>52</sup>*Tokyo Institute of Technology, Tokyo*  
<sup>53</sup>*Tokyo Metropolitan University, Tokyo*  
<sup>54</sup>*Tokyo University of Agriculture and Technology, Tokyo*  
<sup>55</sup>*Toyama National College of Maritime Technology, Toyama*  
<sup>56</sup>*University of Tsukuba, Tsukuba*  
<sup>57</sup>*Virginia Polytechnic Institute and State University, Blacksburg, Virginia 24061*  
<sup>58</sup>*Yonsei University, Seoul*

## Abstract

We present a study of  $Y(4260)$  properties using the initial-state radiation process  $e^+e^- \rightarrow \gamma_{ISR}Y(4260)$ . The  $Y(4260)$  resonance is reconstructed in the  $\pi^+\pi^-J/\psi$  decay mode, using data collected by the Belle detector at the KEKB  $e^+e^-$  collider. We find a significant signal with a central mass value of  $(4295 \pm 10_{-3}^{+10})$  MeV/ $c^2$  and a width of  $(133 \pm 26_{-6}^{+13})$  MeV/ $c^2$ . We find  $\Gamma_{ee} \cdot \mathcal{B}(Y(4260) \rightarrow \pi^+\pi^-J/\psi) = (8.7 \pm 1.1_{-0.9}^{+0.3})$  eV. These results are preliminary.

PACS numbers: 14.40.Gx, 13.66.Bc, 13.25.Gv.

## INTRODUCTION

The  $Y(4260)$  was originally seen by BaBar as a significant enhancement in initial state radiation (ISR) data in the  $\pi^+\pi^-J/\psi$  final state, where it was fitted using a Breit-Wigner function with mass  $(4259 \pm 8_{-6}^{+2}) \text{ MeV}/c^2$  and width  $(88 \pm 23_{-4}^{+6}) \text{ MeV}/c^2$ ; they found  $\Gamma_{ee} \cdot \mathcal{B}(Y(4260) \rightarrow \pi^+\pi^-J/\psi) = (5.5 \pm 1.0_{-0.7}^{+0.8}) \text{ eV}/c^2$  [1]. BaBar have also seen evidence for the decay  $B^- \rightarrow K^-Y(4260)$ ,  $Y(4260) \rightarrow \pi^+\pi^-J/\psi$  [2]. The  $Y(4260)$  has since been confirmed by CLEO in direct production  $e^+e^- \rightarrow Y(4260)$  using energy-scan data [3]; in addition to observing a clear signal in  $\pi^+\pi^-J/\psi$ , CLEO presents evidence for a signal in the  $K^+K^-J/\psi$  and  $\pi^0\pi^0J/\psi$  final states. Recently, CLEO have also presented results using ISR data, where they find a  $Y(4260) \rightarrow \pi^+\pi^-J/\psi$  signal [4]. The  $Y(4260)$  coincides with a minimum in the hadronic cross-section [5] and a minimum in the  $D^*D^*$  cross section [6]; based on a fit to BES data, the authors of Ref. [7] set a lower bound  $\mathcal{B}(Y(4260) \rightarrow \pi^+\pi^-J/\psi) > 0.6\%$ . Such a prominent hadronic transition to  $J/\psi$  is unexpected for a  $c\bar{c}$  state above the  $D^{(*)}\bar{D}^{(*)}$  threshold, and this has led to various other models being proposed. The  $Y(4260)$  has been described as a 4-quark state [8], a molecular state [9, 10, 11, 12], and a quark-gluon hybrid [13, 14, 15, 16]; the possibility that it could be a conventional charmonium state is discussed in Refs [17, 18].

In this paper, we present the results of a search for  $Y(4260) \rightarrow \pi^+\pi^-J/\psi$  production in ISR events. This study is based on a data sample with an integrated luminosity of  $497.1 \text{ fb}^{-1}$  at the  $\Upsilon(4S)$  resonance and  $56.1 \text{ fb}^{-1}$  collected  $60 \text{ MeV}/c^2$  below the resonance. The data were collected with the Belle detector at the KEKB asymmetric-energy  $e^+e^-$  ( $3.5$  on  $8 \text{ GeV}$ ) collider [19].

KEKB operates with a peak luminosity that exceeds  $1.6 \times 10^{34} \text{ cm}^{-2}\text{s}^{-1}$ . The Belle detector is a large-solid-angle magnetic spectrometer that consists of a silicon vertex detector (SVD), a 50-layer central drift chamber (CDC), an array of aerogel threshold Čerenkov counters (ACC), a barrel-like arrangement of time-of-flight scintillation counters (TOF), and an electromagnetic calorimeter comprised of CsI(Tl) crystals (ECL) located inside a superconducting solenoid coil that provides a  $1.5 \text{ T}$  magnetic field. An iron flux-return located outside of the coil is instrumented to detect  $K_L^0$  mesons and to identify muons (KLM). The detector is described in detail elsewhere [20]. Two inner detector configurations were used. A  $2.0 \text{ cm}$  beampipe and a 3-layer silicon vertex detector was used for the first sample of  $155.5 \text{ fb}^{-1}$ , while a  $1.5 \text{ cm}$  beampipe, a 4-layer silicon detector and a small-cell inner drift chamber were used to record the remaining  $397.8 \text{ fb}^{-1}$  [21].

## RECONSTRUCTION

### Monte Carlo and control sample

The ISR process was simulated using Phokhara [22] and events were then ported to qq98 [23], and processed through a simulation of the detector in GEANT [24]. Decays  $Y(4260) \rightarrow \pi^+\pi^-J/\psi$  were simulated using the  $\psi(2S)$  as a model [23]. Events were also generated for the  $\psi(2S)$ , which is being used as a control sample. A data/MC efficiency correction was performed using results from Belle particle identification studies.

## Track Selection

Candidate events are chosen from a standard Belle data skim for hadronic events: the skimming conditions are optimised for  $e^+e^- \rightarrow \Upsilon(4S) \rightarrow B\bar{B}$ , not ISR events. The skimming conditions require the presence of at least three charged tracks ( $N_{\text{ch}} \geq 3$ ), an event vertex with radial ( $r\phi$ ) and  $z$  coordinates within 1.5 and 3.5 cm of the origin, respectively, a total reconstructed energy in the centre-of-mass system (CMS) greater than  $0.2\sqrt{s}$  ( $\sqrt{s}$  is the CMS collision energy), a  $z$  component of the net reconstructed CMS momentum less than  $0.5\sqrt{s}/c$ , a total ECL energy between  $0.1\sqrt{s}$  and  $0.8\sqrt{s}$  with at least two energy clusters, and require  $R_2$ , the ratio of second and zeroth Fox-Wolfram moments, to be less than 0.8. (Here, the  $z$  axis is aligned with the symmetry axis of the detector, and opposite in direction to the  $e^+$  beam. The  $e^-$  beam crosses this axis at an angle of 22 mrad, so the  $e^+e^-$  axis as seen from the CMS is not quite aligned with  $z$ : see the discussion of  $\cos(\theta)$  below.)

We select charged tracks with  $P_t > 0.05 \text{ GeV}/c$  for further analysis. Muons are identified based on track penetration depth and the hit pattern in the KLM system; the selection has an efficiency of 88% for muons. Electron tracks are identified using a combination of  $dE/dx$  from the CDC, ACC information,  $E/p$  ( $E$  is the energy deposited in the ECL and  $p$  is the momentum measured by the SVD and the CDC), and track-cluster matching and shower shape in the ECL; our selection has an efficiency of 92% for electrons. To recover radiated photons from electron candidates, the four-momenta of the closest photon within 0.05 radians of the  $e^+$  or  $e^-$  direction was added to the four-momentum of the track in subsequent analysis. Charged pions are identified as charged tracks that fail electron and muon selection and additionally pass a kaon veto which is applied using energy loss measurements in the CDC, Čerenkov light yields in the ACC, and TOF information. The information from these detectors is combined to form a  $K$ - $\pi$  likelihood ratio,  $\mathcal{R}(K/\pi) = \mathcal{L}_K/(\mathcal{L}_\pi + \mathcal{L}_K)$ , where  $\mathcal{L}_\pi(\mathcal{L}_K)$  is the likelihood that a pion (kaon) would produce the observed detector response. Charged tracks with  $\mathcal{R}(K/\pi) > 0.6$  are vetoed; this selection has an efficiency of 95% for pions, and 13% for kaons.

## Event Reconstruction

We select events with four charged tracks only, then  $J/\psi$  candidates are reconstructed from  $J/\psi \rightarrow \ell^+\ell^-$ , where  $\ell$  is either a positively identified electron or a muon; see Fig. 1 top and bottom, where the curves shown are fits using the Crystal Ball function [25]. The vertical lines indicate the signal and sideband regions,  $|M(\ell^+\ell^-) - m_{J/\psi}| \in [0, 30]$  and  $[90, 150] \text{ MeV}/c^2$  respectively. The  $J/\psi$  candidates are then constrained to a common vertex and the nominal  $J/\psi$  mass [5], to improve the momentum resolution. The perpendicular distance between the  $J/\psi$  vertex and the  $e^+e^-$  interaction point is required to be less than  $100 \mu\text{m}$ . We then reconstruct  $Y(4260)$  candidates by combining the  $J/\psi$  candidates with  $\pi^+\pi^-$  pairs with mass  $M(\pi^+\pi^-) > 0.4 \text{ GeV}/c^2$ . The requirement on  $M(\pi^+\pi^-)$  suppresses the contribution of combinatorial background, including misidentified  $\gamma \rightarrow e^+e^-$  conversions. The recoil mass squared of the  $Y(4260)$  candidates,

$$M_{\text{recoil}}^2 = (\sqrt{s} - E_Y^*)^2 - p_Y^{*2}, \quad (1)$$

is required to satisfy  $|M_{\text{recoil}}^2| < 1 \text{ (GeV}/c^2)^2$ , in accordance with the  $Y(4260)$  being produced via ISR.

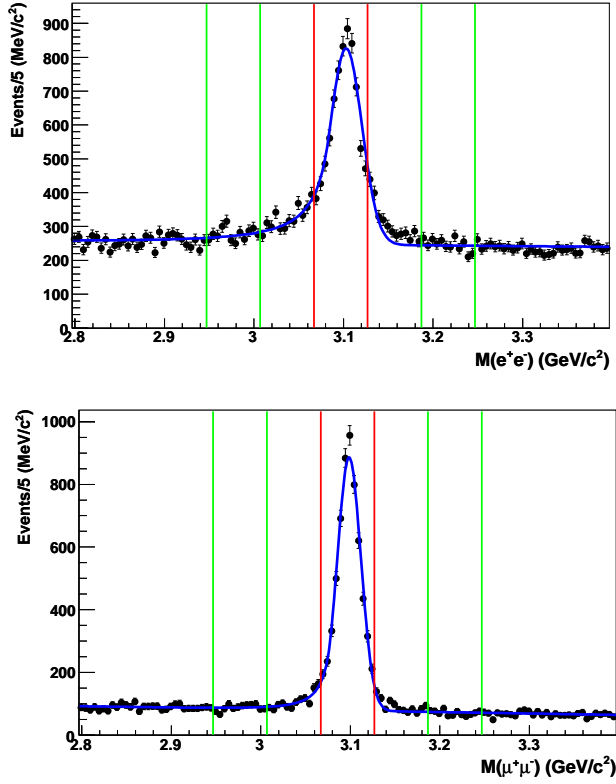


FIG. 1: Invariant mass spectrum of  $J/\psi \rightarrow e^+e^-$  (top) and  $J/\psi \rightarrow \mu^+\mu^-$  (bottom) candidates (points with error bars), and the fit described in the text (solid line). The vertical lines indicate the signal (red) and sideband (green) regions.

The  $\psi(2S)$  is used as a control sample and is reconstructed in the same manner as the  $Y(4260)$  candidates. Squared recoil mass distributions are shown for the sideband subtracted  $Y(4260)$  (Fig. 2) and  $\psi(2S)$  (Fig. 3), and compared with signal MC distributions, where the signal and sideband regions are defined in Table I.

TABLE I: Signal and sideband invariant mass regions.  $\sigma_{\psi(2S)} = 0.012$  is from the wider of the Gaussians fitted to the  $\psi(2S)$  signal.

Region	Mass range ( $\text{GeV}/c^2$ )
$Y(4260)$ Signal	$4.2 < M(\pi^+\pi^- J/\psi) < 4.4$
$Y(4260)$ Sidebands	$3.9 < M(\pi^+\pi^- J/\psi) < 4.0$ $5.1 < M(\pi^+\pi^- J/\psi) < 5.5$
$\psi(2S)$ Signal	$ M(\pi^+\pi^- J/\psi) - 3.686  < 3\sigma = 0.037$
$\psi(2S)$ Sideband	$4\sigma = 0.049 <  M(\pi^+\pi^- J/\psi) - 3.686  < 0.085 = 7\sigma$

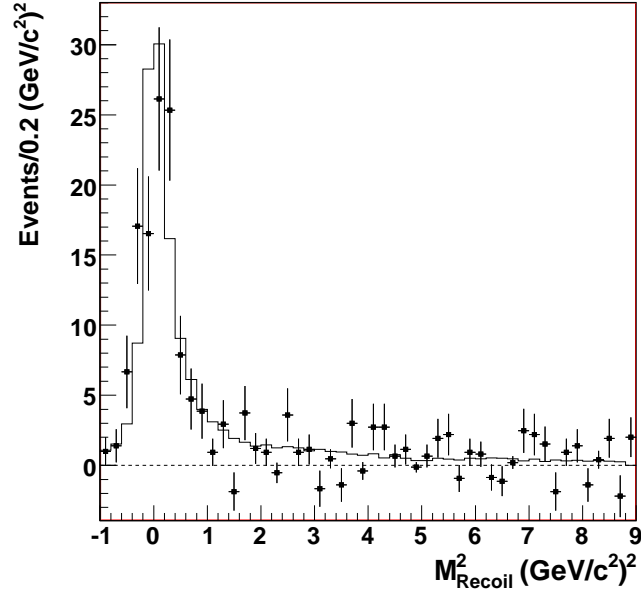


FIG. 2: Recoil mass squared for sideband subtracted  $Y(4260)$  candidates in data (points) and MC (histogram).

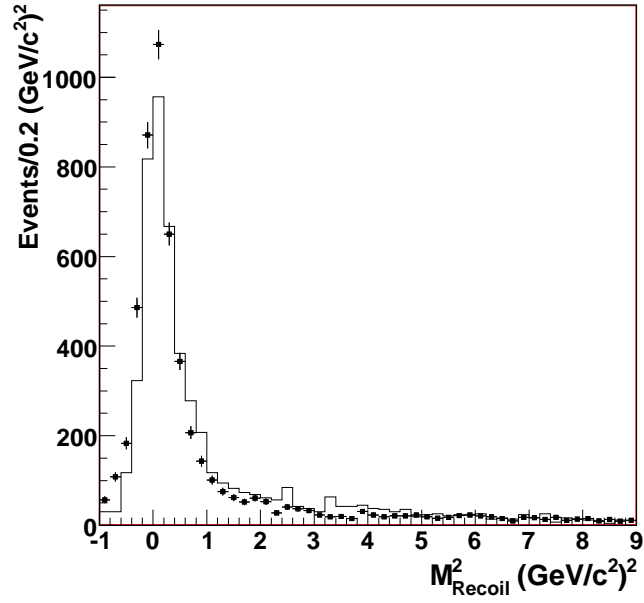


FIG. 3: Recoil mass squared for sideband subtracted  $\psi(2S)$  candidates in data (points) and MC (histogram).

## FIT

We perform a binned maximum likelihood fit to the distribution of invariant mass  $m = M(\pi^+\pi^-J/\psi)$ . The signal function is the product of a Breit-Wigner function, a phase space term, and a mass-dependent efficiency correction, added to a second-order polynomial representing the background. The Breit-Wigner term is

$$\frac{1}{(m - M_Y)^2 + \frac{1}{4}\Gamma^2},$$

the phase space term is

$$\sqrt{((m^2 + m_{J/\psi}^2 - M_{\pi^+\pi^-}^2)/(2m))^2 - m_{J/\psi}^2},$$

and the correction for the efficiency as a function of mass, based on an interpolation of results from  $Y(4260)$  MC samples generated with different central mass values, is

$$a_\epsilon \cdot (m - M_0) + b_\epsilon,$$

where  $M_0 = 4.3 \text{ GeV}/c^2$ ; we fix the parameter  $M_{\pi^+\pi^-} = 0.5 \text{ GeV}/c^2$ . We have neglected the effect of interference with other resonances. The slope and intercept were determined, respectively, to be  $a_\epsilon = (7.4 \pm 1.3) (\text{GeV}/c^2)^{-1}$  and  $b_\epsilon = (9.31 \pm 0.07)$ . The parameters allowed to float in the fit were the number of signal ( $N$ ) events, the mean and width of the Breit-Wigner function ( $M_Y, \Gamma$ ), and the background parameters.

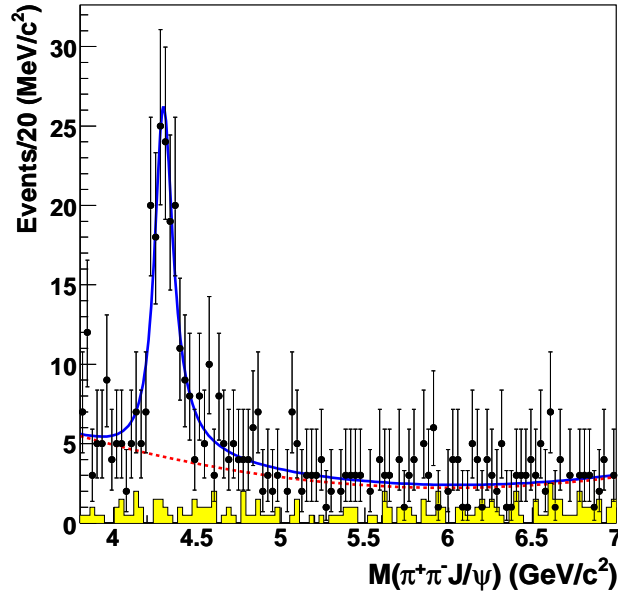


FIG. 4: Invariant mass for  $Y(4260)$  candidates in data (points) and  $J/\psi$  mass sidebands (shaded histogram), with the fit to data (solid line) and its background component (dotted line).

The fit to the data is shown in Fig. 4, together with the (featureless)  $J/\psi$  mass sidebands (shaded histograms). The signal parameters were found to be  $M_Y = (4295 \pm 10_{-3}^{+10}) \text{ MeV}/c^2$ ,



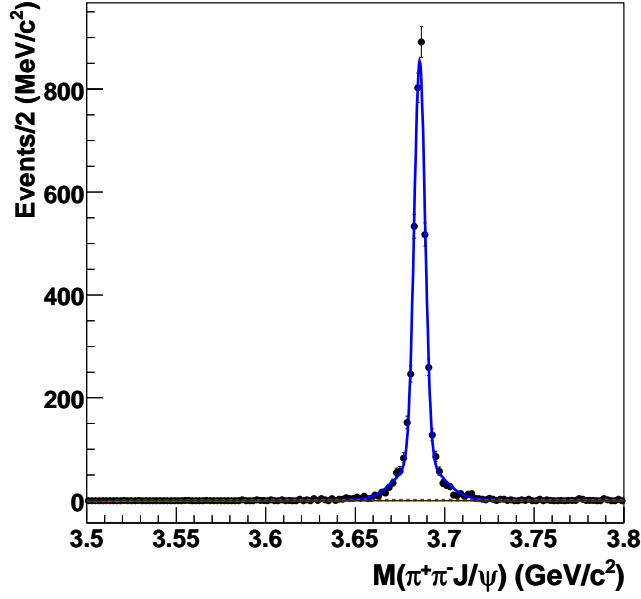


FIG. 5: Invariant mass for  $\psi(2S)$  candidates in data (points), with the fit to data (solid line) and its background component (dotted line).

$\Gamma = (133 \pm 26_{-6}^{+13}) \text{ MeV}/c^2$  with a yield  $N = (165 \pm 24_{-23}^{+7})$  events, where the systematic terms will be described in the next section. The significance of this signal was estimated by comparing fits with and without a signal term and was found to be  $11\sigma$ .

The  $\psi(2S)$  control sample was fitted using two Gaussians and a bifurcated Gaussian, with a common mean  $M_{\psi(2S)}$  floating in the fit, and a linear background: see Fig. 5. Using the Particle Data Group value of  $\Gamma_{ee}(\psi(2S))$  [5] we expect our  $\psi(2S)$  yield to be  $4575 \pm 290$ , where the error is dominated by MC statistics. We observe a  $\psi(2S)$  yield of  $4188 \pm 67$ , where the error is statistical only.

### ISR photon reconstruction

Photons are identified as ECL energy clusters that are not associated with a charged track and have a minimum energy of 0.060 GeV. If the photon with highest energy  $E_{\gamma_{ISR}}$  in an event satisfies  $E_{\gamma_{ISR}} + E_{(\pi^+\pi^-J/\psi)} > 10 \text{ GeV}$  then the ISR photon is considered to be reconstructed. The  $Y(4260)$  candidates that pass this criteria are shown in Fig. 6; an enhancement is seen at  $M(\pi^+\pi^-J/\psi) \approx 4300 \text{ MeV}/c^2$ .

## PROPERTIES

### Dipion Mass

Figure 7 shows the efficiency-corrected dipion mass distribution for  $Y(4260)$  candidates with the prediction from MC, based on fits to  $M(\pi^+\pi^-J/\psi)$  in  $M(\pi^+\pi^-)$  bins. The effect of the  $\pi^+\pi^-J/\psi$  mass threshold that is introduced by the  $M(\pi^+\pi^-)$  binning is taken into

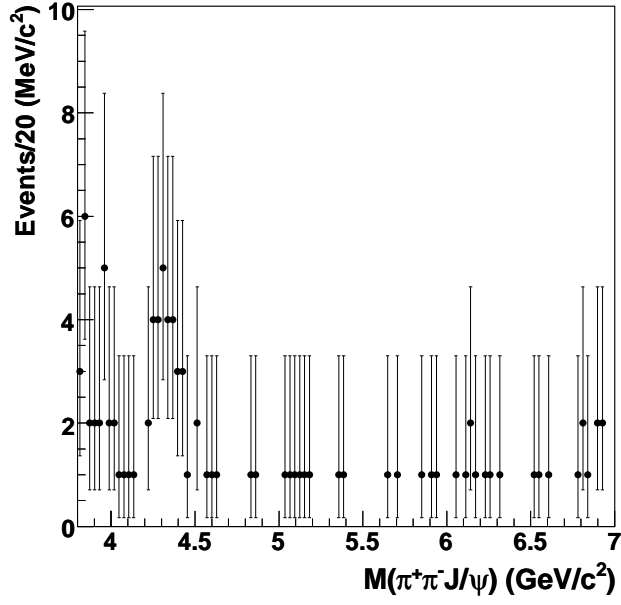


FIG. 6:  $Y(4260)$  invariant mass spectrum requiring reconstruction of the ISR photon.

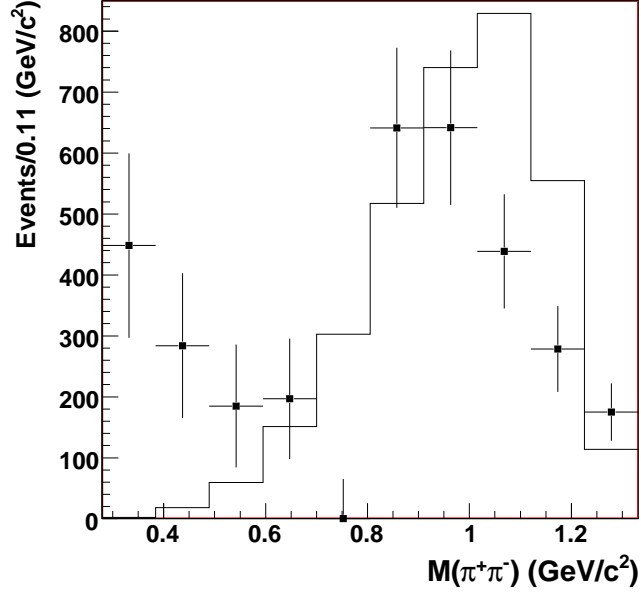


FIG. 7: Invariant mass of  $\pi^+\pi^-$  combinations in  $Y(4260)$  candidates from fitted yields, after efficiency correction in data (points) and MC (histogram).

account by multiplying the signal and background terms by an appropriate threshold function in each bin. Both signal and background parameters are fixed from the fit to the full sample, and only the normalisation and threshold function terms are allowed to vary. The yield ( $n_i$ ) in each bin is corrected using the efficiency ( $\epsilon_i$ ), calculated in the same bin using  $Y(4260)$  MC.

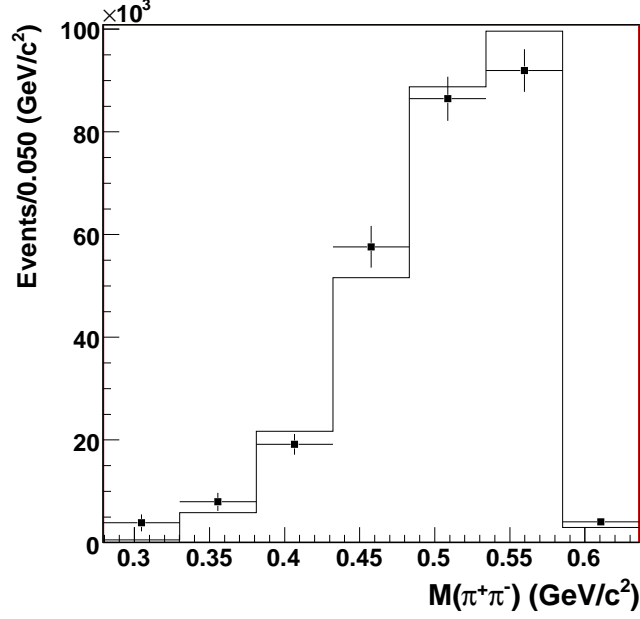


FIG. 8: Invariant mass of  $\pi^+\pi^-$  combinations in  $\psi(2S)$  candidates, after efficiency correction in data (points) and MC (histogram).

The  $\psi(2S)$  dipion mass distribution in Fig. 8 is corrected using a 2nd order polynomial fit to the binned efficiency from MC produced at the nominal  $\psi(2S)$  mass, the errors are dominated by the MC error in the binned efficiencies.

#### $\cos(\theta)$ distribution

Figure 9 shows the efficiency-corrected  $\cos(\theta)$  distribution for  $Y(4260)$  candidates with the prediction from MC, where  $\theta$  is the polar angle of  $Y(4260)$  candidates relative to the direction of the  $e^-$  beam, as seen from the CMS.  $M(\pi^+\pi^-J/\psi)$  fits are performed in  $\cos(\theta)$  bins, with signal and background parameters fixed from the fit to the full sample, and only the normalisation terms allowed to vary. The yield in each bin is corrected using the efficiency calculated in the same bin, based on the  $Y(4260)$  MC as above. Smaller bins were used close to  $\cos(\theta) = \pm 1$ , where the efficiency is changing rapidly, and then combined for the final plot. The same procedure was followed to produce the  $\cos(\theta)$  plot in the  $\psi(2S)$  reference channel, Fig. 10.

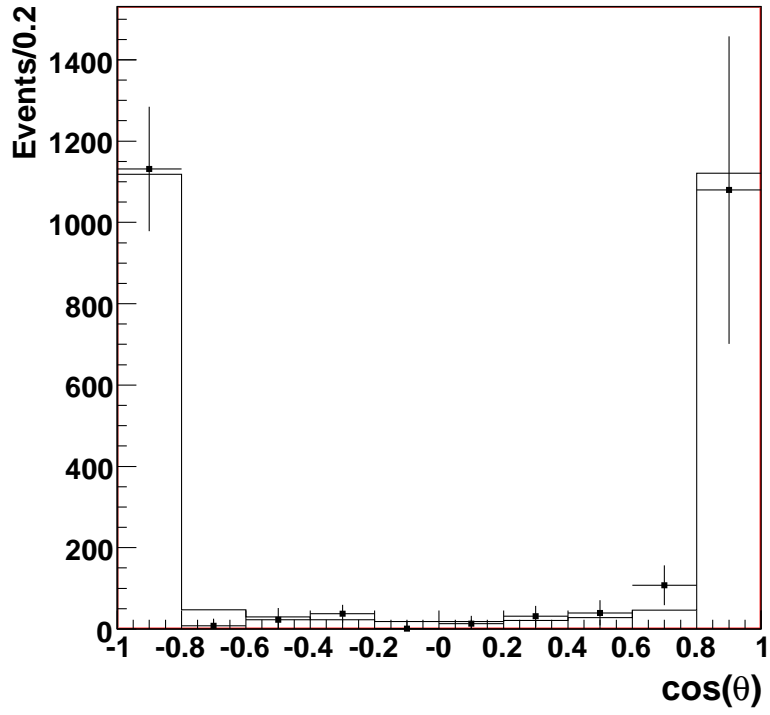


FIG. 9: Efficiency corrected  $\cos(\theta)$  distribution for  $Y(4260)$  candidates in data (points) and MC (histogram).

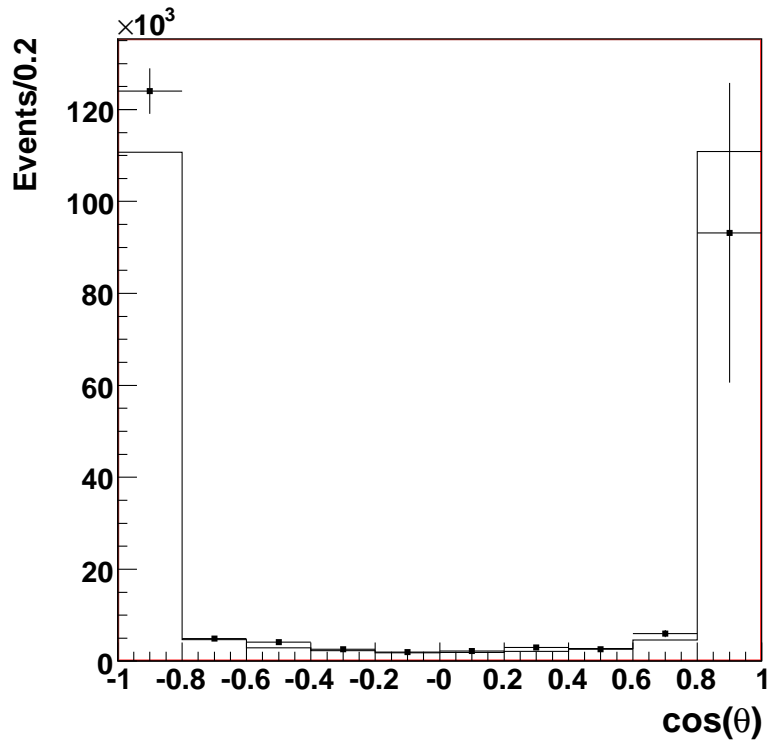


FIG. 10: Efficiency corrected  $\cos(\theta)$  distribution for  $\psi(2S)$  candidates in data (points) and MC (histogram).

## SYSTEMATICS

The systematic uncertainties on the mass and width measurement were estimated by varying the fitting procedure. Variant fits including signal functions without phase space and efficiency corrections, a linear background shape, 10 MeV/ $c^2$  binning, and a (3.8,5.0) GeV/ $c^2$  fit range were performed, and the largest deviations were taken as the positive and negative systematic errors due to fitting. We then add in quadrature terms from possible biases in  $Y(4260)$  mass reconstruction (based on a fit to MC) and the overall mass scale (using the  $\psi(2S)$  for calibration). The fitting function does not take the variation with mass of the ISR cross-section into account. We estimate the resulting error in  $\Gamma_{ee} \cdot \mathcal{B}$  (see the next section) using the relative change in the second-order QED radiator  $W(s, x)$  [26] as the  $\pi^+\pi^- J/\psi$  mass is changed from the fitted mean value by  $\pm 1\Gamma$ . ( $x \equiv 2E_\gamma/\sqrt{s}$ , where  $E_\gamma$  is the energy of the ISR photon in the CMS.) A summary of systematic error terms can be found in Table II.

TABLE II: Sources of systematic error.

Source	Mass (MeV/ $c^2$ )	Width (MeV/ $c^2$ )	$\sigma \cdot \mathcal{B}$ (fb)	$\Gamma_{ee} \cdot \mathcal{B}$ (eV)
Fitting procedure	$+10$ $-2$	$+13$ $-6$	$+1$ $-5$	$+0.2$ $-0.9$
Measurement of mass in $Y(4260)$ MC	$\pm 2$	—	—	—
Mass scale from measurement of $\psi(2S)$	$\pm 2$	—	—	—
QED radiator at masses of $\pm 1\Gamma$	—	—	—	$\pm 0.2$
Total	$+10$ $-3$	$+13$ $-6$	$+1$ $-5$	$+0.3$ $-0.9$

Additional fits were conducted on the di-electron and di-muon samples independently and found to be consistent with the combined result.

## CROSS SECTION

Taking the fitted  $Y(4260)$  yield  $n_i$  and the efficiency  $\epsilon_i$  in bins of dipion mass, as described above, we identify

$$\sum \frac{n_i}{\epsilon_i} = \int dt \mathcal{L} \cdot \sigma(e^+e^- \rightarrow \gamma_{ISR} Y(4260); \sqrt{s} = 10.58) \cdot \mathcal{B}(Y(4260) \rightarrow \pi^+\pi^- J/\psi) \cdot \mathcal{B}(J/\psi \rightarrow \ell^+\ell^-). \quad (2)$$

The use of  $M(\pi^+\pi^-)$  bins reduces the model dependence of the result at the cost of increasing the statistical error. Substituting the world average value for  $\mathcal{B}(J/\psi \rightarrow \ell^+\ell^-)$  [5], we find

$$\sigma(e^+e^- \rightarrow \gamma_{ISR} Y; \sqrt{s} = 10.58) \cdot \mathcal{B}(Y(4260) \rightarrow \pi^+\pi^- J/\psi) = (48 \pm 6_{-5}^{+1}) \text{ fb}.$$

Using equation (7) from Ref. [26] we calculate, in the small width approximation,  $\Gamma_{ee} \cdot \mathcal{B}(Y(4260) \rightarrow \pi^+\pi^- J/\psi) = (8.7 \pm 1.1_{-0.9}^{+0.3}) \text{ eV}$ .

From the signal function of a fit to the full sample (without applying an  $M(\pi^+\pi^-)$  cut) we find the cross-section at the peak value of 4.295 GeV/ $c^2$  for  $e^+e^- \rightarrow Y(4260) \rightarrow \pi^+\pi^- J/\psi$  to be 43 pb.

## DISCUSSION

We have confirmed the  $Y(4260) \rightarrow \pi^+\pi^- J/\psi$  signal with a significance of  $11\sigma$ . The dipion mass distribution favours high values of  $M(\pi^+\pi^-)$ , which is consistent with BaBar's result; there is also some evidence for a rise in cross-section near the  $M(\pi^+\pi^-)$  threshold, although statistical errors are large. The  $\cos(\theta)$  distribution peaks strongly at values near  $\pm 1$ , consistent with the interpretation that the events are due to ISR, and when we require the reconstruction of the ISR photon we see an enhancement near the central mass value.

For our signal we find a mass of  $(4295 \pm 10_{-3}^{+10})$  MeV/ $c^2$ . There have been predictions that a hybrid would favour decays to an  $S$ -wave plus a  $P$ -wave state [27]; the relevant mass threshold is  $M(D^0 D_1^0) = 4287$  MeV/ $c^2$ . We find a mass above this value, although the difference is not statistically significant. CLEO's preliminary measurement is  $(4283_{-16}^{+17} \pm 4)$  MeV/ $c^2$ , coinciding with the threshold and consistent with our value; BaBar's published mass is  $(4259 \pm 8_{-6}^{+2})$  MeV/ $c^2$ , below threshold and  $2.6\sigma$  below our value. Our measurement of the width,  $\Gamma = (133 \pm 26_{-6}^{+13})$  MeV/ $c^2$  is consistent with those of CLEO  $(70_{-25}^{+40} \pm 5)$  MeV/ $c^2$  and BaBar  $(88 \pm 23_{-4}^{+6})$  MeV/ $c^2$ ; errors are large. Our result for  $\Gamma_{ee} \cdot \mathcal{B}(Y \rightarrow \pi^+\pi^- J/\psi)$  is about  $1.6\sigma$  higher than BaBar's reported value  $(5.5 \pm 1.0_{-0.7}^{+0.8})$  eV/ $c^2$ .

## SUMMARY

We have investigated the properties of the  $Y(4260)$  using the initial-state radiation process  $e^+e^- \rightarrow \gamma_{ISR} Y(4260)$ . We observe a significant signal described by a Breit-Wigner with mass  $(4295 \pm 10_{-3}^{+10})$  MeV/ $c^2$  and width  $(133 \pm 26_{-6}^{+13})$  MeV/ $c^2$ , and find  $\Gamma_{ee} \cdot \mathcal{B}(Y(4260) \rightarrow \pi^+\pi^- J/\psi) = (8.7 \pm 1.1_{-0.9}^{+0.3})$  eV. These results are preliminary.

## ACKNOWLEDGEMENTS

We thank the KEKB group for the excellent operation of the accelerator, the KEK cryogenics group for the efficient operation of the solenoid, and the KEK computer group and the National Institute of Informatics for valuable computing and Super-SINET network support. We acknowledge support from the Ministry of Education, Culture, Sports, Science, and Technology of Japan and the Japan Society for the Promotion of Science; the Australian Research Council and the Australian Department of Education, Science and Training; the National Science Foundation of China and the Knowledge Innovation Program of the Chinese Academy of Sciences under contract No. 10575109 and IHEP-U-503; the Department of Science and Technology of India; the BK21 program of the Ministry of Education of Korea, the CHEP SRC program and Basic Research program (grant No. R01-2005-000-10089-0) of the Korea Science and Engineering Foundation, and the Pure Basic Research Group program of the Korea Research Foundation; the Polish State Committee for Scientific Research; the Ministry of Science and Technology of the Russian Federation; the Slovenian Research Agency; the Swiss National Science Foundation; the National Science Council and the Ministry of Education of Taiwan; and the U.S. Department of Energy.

- 
- [1] B. Aubert *et al.* (BaBar collaboration), Physical Review Letters **95**, 142001 (2005).
  - [2] B. Aubert *et al.*, Physical Review D **73**, 011101 (2006).
  - [3] T.E. Coan *et al.* (CLEO collaboration), Physical Review Letters **96**, 162003 (2006).
  - [4] Q. He *et al.* (CLEO Collaboration), hep-ex/0611021 (2006); submitted to Physical Review D as a Rapid Communication.
  - [5] W.-M. Yao *et al.* (Particle Data Group), Journal of Physics G **33**, 1 (2006).
  - [6] K. Abe *et al.* (Belle Collaboration), hep-ex/0608018 (2006).
  - [7] X. H. Mo *et al.*, Physics Letters B **640**, 182 (2006).
  - [8] L. Maiani, F. Piccinini, A. D. Polosa, and V. Riquer, Physical Review D **72**, 031502 (2005).
  - [9] T. C. T.-W. Chiu and T.-H. Hsieh, Physical Review D **73**, 094510 (2006).
  - [10] C. Z. Yuan, P. Wang, and X. H. Mo, Physics Letters B **634**, 399 (2006).
  - [11] C.-F. Qiao, Physics Letters B **639**, 263 (2006).
  - [12] X. Liu, X.-Q. Zeng, and X.-Q. Li, Physical Review D **72**, 054023 (2005).
  - [13] S.-L. Zhu, Physics Letters B **625**, 212 (2005).
  - [14] F. E. Close and P. R. Page, Physics Letters B **628**, 215 (2005).
  - [15] E. Kou and O. Pene, Physics Letters B **631**, 164 (2005).
  - [16] X.-Q. Luo and Y. Liu, Physical Review D **74**, 034502 (2006).
  - [17] E. van Beveren and G. Rupp, hep-ph/0605317, 2006.
  - [18] F. J. Llanes-Estrada, Physical Review D **72**, 031503 (2005).
  - [19] S. Kurokawa and E. Kikutani, Nuclear Instruments and Methods A **499**, 1 (2003), and other papers included in this volume.
  - [20] A. Abashian *et al.* (Belle Collaboration), Nuclear Instruments and Methods A **479**, 117 (2002).
  - [21] Z. Natkaniec *et al.* (Belle SVD2 Group), Nuclear Instruments and Methods A **560** 1 (2006).
  - [22] H. Czyz *et al.*, European Physics Journal C **47**, 617 (2006).
  - [23] <http://www.lns.cornell.edu/public/CLEO/soft/QQ/>.
  - [24] R. Brun *et al.*, GEANT 3.21, CERN Report DD/EE/84-1 (1984).
  - [25] T. Skwarnicki, Ph.D. Thesis, Institute for Nuclear Physics, Krakow 1986; DESY Internal Report, DESY F31-86-02 (1986).
  - [26] M. Benayoun *et al.*, Modern Physics Letters A **14**, 2605 (1999).
  - [27] S. Godfrey, hep-ph/0605152, 2006.